

Brain morphometry by distance measurement in a non-Euclidean, curvilinear space

Martin Styner¹, Thomas Coradi² and Guido Gerig¹

¹Dept. of Computer Science, University of North Carolina at Chapel Hill, USA

²Communication Technology Lab, Image Science, ETH-Zurich, Switzerland email: {styner,gerig}@cs.unc.edu,tcoradi@vision.ee.ethz

Abstract

Inspired by the discussion in most recent neurological research about the role of callosal fiber connections with respect to brain asymmetry [1, 2] we developed a technique that can measure distances between brain hemispheres in a non-Euclidean, curvilinear space. The new technique is a generic morphometric tool for measuring minimal distances within and across 3-D structures, but the project described herein is focused on assessing brain asymmetry in schizophrenia research. We use segmented brain white matter as a mask and measure distances from the cortical gray/white matter boundary to the cross-section of the corpus callosum through white matter tissue. The midsagittal cut through the corpus callosum serves as a symmetry center between the two hemispheres. The method uses a 3-D extension of a graph search algorithm, called F^ . We search for minimum cost paths between a seed point or a seed region, respectively, and all the other points in space, constrained by the mask acting as a cost matrix. The algorithm is not limited to binary masks but allows us to use the original inhomogeneity-corrected MR volume with appropriate transfer function as a cost matrix. The resulting distances are mapped to the cortical surface and differences on the two hemispheres can be visually compared. Distances were also projected back to the corpus callosum along their minimum cost trajectories to represent asymmetry by comparing left and right measurements. Whereas a comparison between homologous points and regions on each hemisphere and thus a complete brain asymmetry map is still in development, we can present preliminary results obtained by processing 11 3-D magnetic resonance data sets representing a normal control group.*

1. Introduction

Imaging and image analysis has become a common component to study diseases of the human body by obtaining anatomical and functional information. Image processing techniques can derive quantitative morphometric measurements of the size and shape of biological structures. Morphometry has become increasingly important since the advent of non-invasive magnetic resonance imaging which is providing large volumes of data from normal as well as abnormal individuals in vivo and even allows time changes to be studied. However, image analysis is still a limiting factor in most clinical studies due to the lack of automated and efficient tools for accurate and reproducible segmentation of large amounts of 3-D image data sets. The new analysis methodology described in this article is a fully 3-D processing technique and overcomes limitations of conventional slice-by-slice analysis.

1.1. Driving clinical research project

This project is driven by studying schizophrenia, a disease of great economic, social and medical importance. In schizophrenia, changes in the morphology of various brain structures are thought to provide important clues to the most fundamental brain abnormalities that underlie the condition, but the changes are subtle and barely be detectable with current interactive segmentation techniques [3, 4]. Here, the need for improved morphometric techniques is particularly clear. Computational techniques applied to 3-D magnetic resonance images mostly explore the question to find brain abnormalities and the areas of the brain that are affected, to relate such abnormalities to clusters in schizophrenia, and to answer related questions like the specificity and the etiology of such brain abnormalities.

Quantitative measurements on postmortem brains and on anatomical structures segmented from magnetic resonance image data corroborate the hypothesis that the asymmetry between the brain hemispheres is reduced at first episodes of schizophrenia [5, 6]. To date, the errors in measurements are often larger than the effect to be studied, and interesting findings often could not be confirmed by other research groups. Therefore, it becomes necessary to provide new and more accurate measurements of brain asymmetry. Bullmore et al. [7] proposed a measurement called *radius of gyration* to assess cerebral asymmetry. This measurement, however, has been only applied to 2-D coronal slices of 3-D brain images. Prima et al. [8] applied non-linear elastic registration to find corresponding regions in the two hemisphere. Differential operators applied to the 3-D deformation field results in measures of lateral asymmetry.

1.2. Measurement and assessment of asymmetry in 3-D space

Symmetry of structures to mean exact equality under a class of spatial transformations is a well-defined mathematical property. However, dealing with biological structures and the inherent variability, the mathematical approach to exact symmetry is too strict. The intrinsically binary definition has to be changed for medical applications, as we have deal with elastically deformable objects which are “symmetric” about a curved axis, for example. Further, we might be interested in calculating the degree of symmetry to compare anatomical structures.

Guillemaud et al. [6] segmented the manifold of the interhemispheric fissure and determined length between the cortical surface and the fissure along perpendicular lines emanating from the midplane. Measures from the left and right cortical surface collected at the midplane result in estimates of local asymmetries and in a quantitative 2-D asymmetry map. This paper also suggested the use of a curvilinear coordinate system of the brain directly related to brain morphology. Trajectories of the curvilinear coordinate system have a rough similarity to brain connectivity by providing a kind of simulation of transcallosal white matter fibers. The encouraging results inspired the research work presented in this paper. We have to clarify that the trajectories between brain hemispheres and the cross-section of the corpus callosum derived by the dynamic search technique are used as a means for measuring distances in a curvilinear coordinate system. A more realistic simulation of white matter fiber connections, however, would have to include information about local fiber directions, as nicely presented in [9] and [10], for example. The search for minimum cost paths is an 3-D extension of the F^* algorithm [11] and has similarities to the interactive live-wire segmentation systems presented in [12, 13]. In the context of analyzing the white matter structure of the brain we also would like to refer to Mangin et al. [14] who proposed a discrete implementation of conservative flow systems to analyze the white matter network of the brain, in particular to automatically detect the corpus callosum which forms a bottleneck in

information flow.

2. Methods

In our proposed approach, callosal fibers are simulated by curvilinear paths of minimal distance running inside the white matter from the white matter boundary to the interhemispheric cut through the corpus callosum. We use distance measurements propagated along trajectories determined by a graph search algorithm. The original F^* algorithm, known from dynamic programming, has been extended in several ways to fit our specific needs. The result of the application of F^* to a dataset is a 3-D distance map which is used to trace back the paths by a steepest descent approach. The distances at the white matter boundary can then be projected back onto the corpus callosum along these paths for a comparison of asymmetry between the two hemispheres.

2.1. Optimal path algorithm

The F^* -algorithm used in our implementation is based on the approach of Tenenbaum [11], where pixels or voxels of a dataset are represented by nodes of a graph. The edges of the graphs are defined as the 8-neighborhood in 2-D space and as the 26-neighborhood in 3-D space. The F^* -algorithm enables the calculation of a distance map from a certain point of reference ('seed') to any other point in the graph. This distance map assigns a distance-value to each node in the graph which is based on a cost function that determines the point-related cost of a path. The distance at a node is equal to the sum of the costs on the optimal path to the seed point. A path is considered optimal if there exists no other path of smaller distance. The F^* -algorithm determines the distance map without explicitly calculating the optimal paths. However, the optimal path is implicitly coded in the calculated distance map and can therefore be extracted.

Starting from a distance map that consists of the value zero for the seed point and the value 'infinity' for all other points, the algorithm refines the distance map iteratively until there are no more refinements to be done. Every iteration consists of distinct phases. For the 2-D case the first phase is a left-right/top-bottom scan. After the processing of each line, the distance map is updated in a second phase running from right to left. Step three and four are scans running from right-left/bottom-top and left-right, respectively. In each of these 4 phases, the distance value of a point is updated by the minimum computed over its old value and the distance values of the points of a masked neighborhood, each attributed with the cost of the actual point. The neighborhood mask consists of those points from the 8-neighborhood that have been already processed in this scan.

2.2. Extensions of F^*

To fit our needs we have implemented several extension of the original F^* algorithm:

- The extension of F^* to 3-D space is straightforward. There are 6 phases instead of 4, including two additional phases for front-back and for back-front scanning.
- The seed for the calculation of the distances is in our application the cross-section of the corpus callosum, which isn't just a single point but a 3-D manifold. The algorithm was therefore extended to use a seed region instead of a single seed point by initializing every point that is part of the seed region to zero. This also allows multiple seed regions to be specified (see Figure 1).

- The algorithm was also modified to determine appropriate costs (measured in unit size) for paths running along diagonals, which are weighted by a factor of $\sqrt{2}$ for in-slice diagonals and $\sqrt{3}$ for out-of-slice diagonals. This is of course just the case for an isotropically sampled dataset with unit voxel size. Each direction needs additional correction if voxel dimensions are non uniform.
- Propagation of additional information and measurements from the corpus callosum to all points of the white matter structure can be done at the same time the minimal distance is calculated.

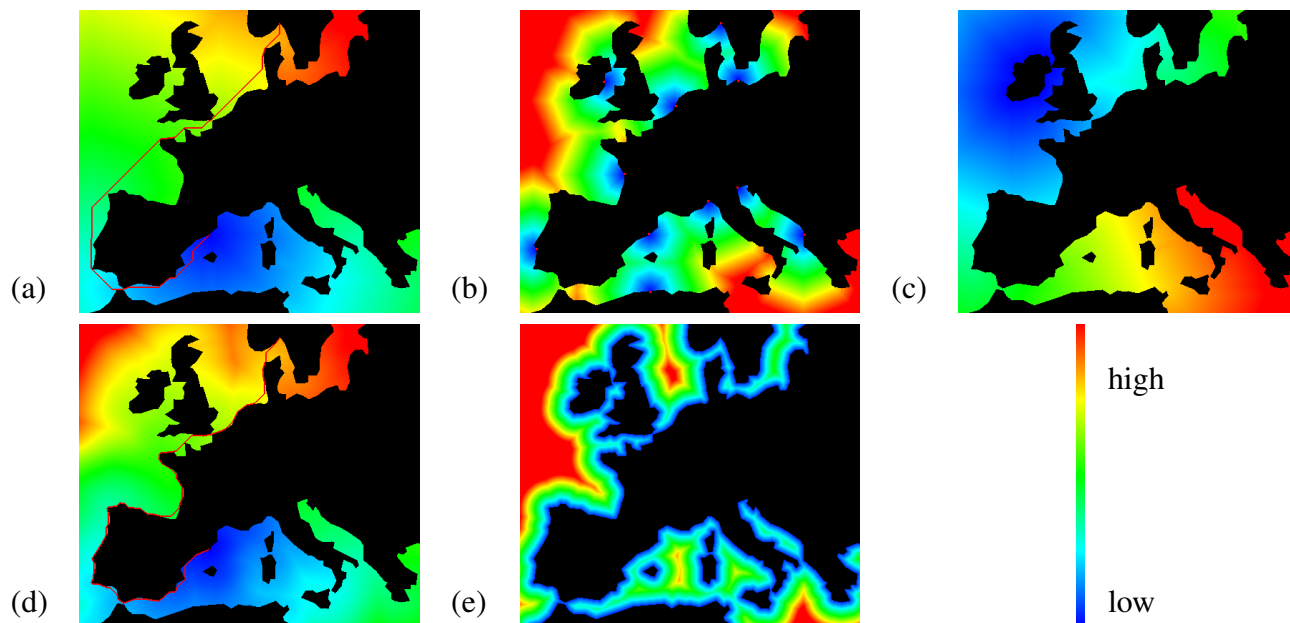


Figure 1. 2-D F^* distance maps representing the distance of the sea route to the closest seed point: (a) single seed point (at Barcelona) with highlighted optimal path running to Stockholm, (b) multiple seed points, (c) seed region (border of Ireland), (d) single seed, costmatrix penalizing optimal paths running far off the coast, with highlighted optimal path as in (a). (e) Visualization of penalty term for (d).

2.3. Calculation of cost matrices

The F^* algorithm needs the cost function to be stored as a matrix ('costmatrix') which has the same dimensions as the original dataset and represents the point-related costs for each point. In our first approach a value of 1 is assigned to all points. This way the resulting distance map represents the path lengths measured in unit size (commonly millimeters), which is a property that is highly desirable for an appropriate distance measurement.

In a second approach, the cost matrix was modeled to force optimal paths to run less likely through certain regions. We modeled the cost matrix by two terms, one term for the distance, which is constantly 1, and a penalty-term to assign high costs to points where paths should be less likely to run through (see Figure 1). The path lengths and therefore the propagated distances using such a costmatrix are no longer measured in the amounts of unit size, requiring a modification of the F^* algorithm. Additionally to the

accumulated costs a second attribute is stored at each point in the dataset, which represents the distance in unit size. This value is updated at the same time as the accumulated costs, but not used to determine the optimal path. Similarly, other attributes can be calculated and propagated. For example, all seed points are labeled and this label gets propagated through the dataset during the calculation of F^* . The label stored at each point then represents the closest seed point.

We have implemented two versions using cost matrices based on local image information. The penalty term is reciprocal to the probability of the presence of a path (see Figure 2). Since in our application we are looking for a rough model of white matter tracts, we have set this probability equal to the probability of the presence of white matter. The first cost matrix is based on a one-class Gaussian tissue model. The second, more sophisticated approach is based on the a-posteriori probability for white matter (see Figure 2), which is derived from a statistical Bayesian classification using the classes cerebro-spinal fluid, white and gray matter. The resulting paths vary only slightly between the two probability models.

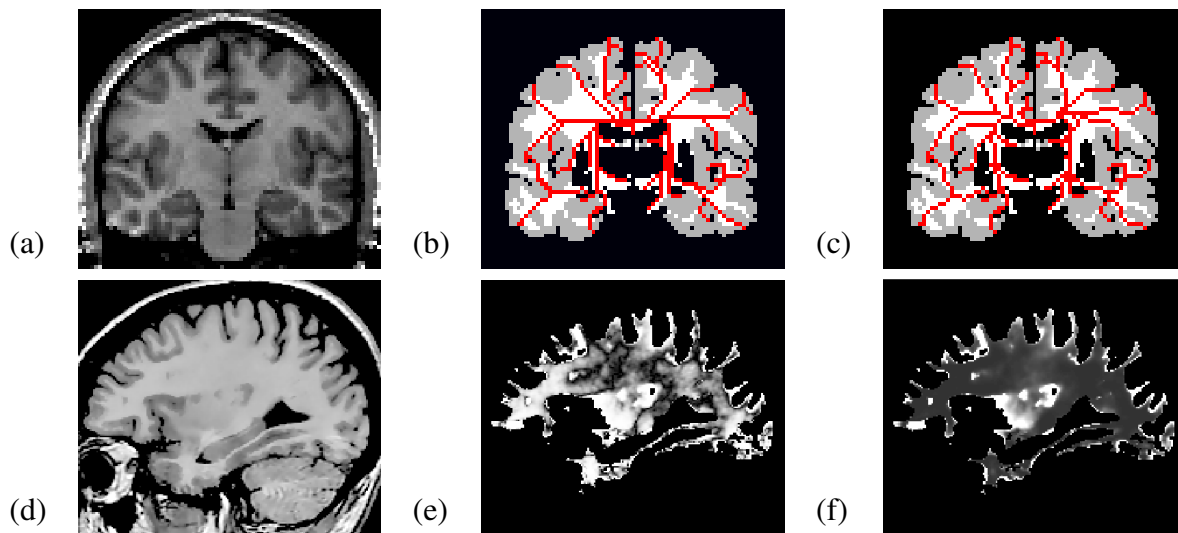


Figure 2. Image data based cost matrices (in 2-D): original images (a) + (d). Visualization of arbitrary optimal paths based on a constant cost matrix (b) and based on an a-posteriori probability cost matrix (c). Cost matrix of the one-class tissue model (e) and of the a-posteriori probability model (f) (high cost \rightarrow high grayvalue).

2.4. Reconstruction of the optimal path

The optimal path is not an explicit result of the F^* algorithm. Its reconstruction can either be done by extending the F^* to store the minimal direction at every point or by extracting it from the distance map using a steepest descent approach to trace trajectories back to the seed points. In our implementation the latter method was used. Visualization of paths are shown in figures 2 and 3.

2.5. Projection of white matter distance to cortical surface

So far, we have calculated distances at the white matter boundary. However such a visualization is rather unusual and requires training. More common is a projection of attributes to the cortical surface, which

also allows a comparison between multiple brain surfaces.

We have developed a method to project the calculated distances from the gray/white matter boundary outwards to the cortex through gray matter using the F^* algorithm. Paths are allowed to run through gray matter. All gray matter areas have the same cost, which is chosen considerably high so that there are no shortcuts through gray matter for any optimal white matter path. We perform F^* twice on the dataset, once with the present cost matrix and once with the modified cost matrix that has double costs in the white matter area. The resulting distance map of the subtraction of these two is the desired distance map that has the distance values projected out to the cortex. The projection is done along the optimal path running from the white matter boundary to the cortex. A point on the cortex is assigned the distance value of the closest point at the white matter boundary along optimal paths in the gray matter (see Figure 3).

2.6. Asymmetry analysis by back-projection of distances to the corpus callosum

The main problem in defining asymmetry measurements is to determine correspondence. Establishing correspondence between brain hemispheres is tackled by several research groups, e.g. [8], but is not well defined since the brain is not strictly symmetric and depicts structures which appear only in one hemisphere. The approach chosen in our application is to project the distances back to the corpus callosum along optimal paths, where an implicit correspondence is already given. Every point of the corpus callosum can be looked at as to belong to both hemispheres at the same time. Measurements projected from both sides to one point of the corpus callosum can therefore be compared directly for asymmetry.

We define our asymmetry measurement as the difference of the mean of the distances projected to each unit area on the corpus callosum. A point on the corpus callosum collects the values of all endpoints of optimal paths having its origin at this point. After averaging the collections of distance values separately for each side, the differences of the means are determined. These differences can be visualized as a 2-D difference graph or can be projected again back to the cortex for visualization. For a more robust and less noisy measurement we apply a low-pass filtering on the means and on the differences.

3. Applications and Results

The proposed algorithm has been applied on 2-D datasets without symmetry axis like maps (see Figure 1) and mazes to test and extend the functionality of the F^* algorithm. Further 2-D tests involved datasets with symmetry axis at the seed region, like artificial images, images of butterflies, bats, plants and 2-D-slices of a brain atlas. In these tests the proposed correspondence and several modifications of the asymmetry measurement were tested and refined. The mean distance asymmetry measure showed to be superior to extrema or median measures. Corresponding catchment areas of a point on the symmetry axis showed high variability in cases when areas were hidden behind obstacles. In such cases the correspondence and thus the asymmetry measurement turned out to be poor.

The first 3-D test has been performed on an isotropic (1.875 x 1.875 x 1.875 mm) brain atlas. The applied cost matrix is based on a one-tissue-model of the white matter. Distances and paths were calculated and visualized (Figures 2(a-c), 3). There were significant visual differences observed between the two hemispheres. The difference graph of the mean was determined as asymmetry measurement and visualized (Figure 4). Both the asymmetry graph and the distance visualization on the cortex demonstrate that the left hemispheric paths are longer for most parts of the brain. Compared to the 2-D case, we

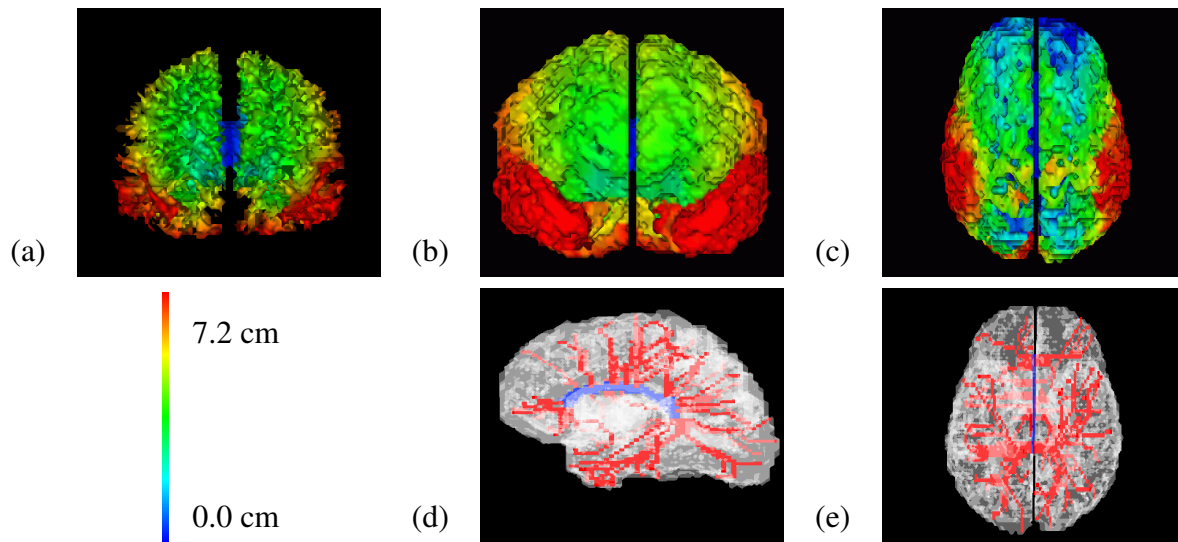


Figure 3. Application on a 3-D brain atlas. Visualization of calculated distances on the white matter boundary (a) and as projection to the cortex from anterior (b) and inferior (c) viewpoints. Visualization of paths (red) and corpus callosum (blue) in 3-D from left (d), and superior (e) viewpoints.

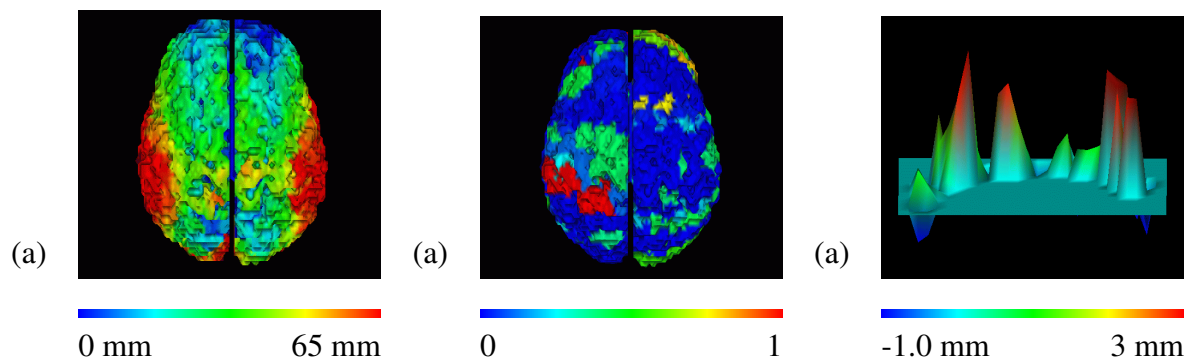


Figure 4. Application on a 3-D brain atlas. Visualization of distances (a) and of normalized asymmetry measurement (b) as a projection on the cortex. Areas of smaller or equal mean distance than their corresponding areas on the other hemisphere are displayed in blue. (c) Visualization of the difference graph (left minus right) projected onto the 2-D cut through the corpus callosum. The lower left point of the graph is located anatomically posterior and inferior.

observed a lower variance of the size of catchment areas, but nevertheless the correspondence was not solved to our full satisfaction. One reason might be that the corpus callosum is a rather small structure compared to the size of the white matter boundary, so rather large areas can be projected onto a single point on the corpus callosum.

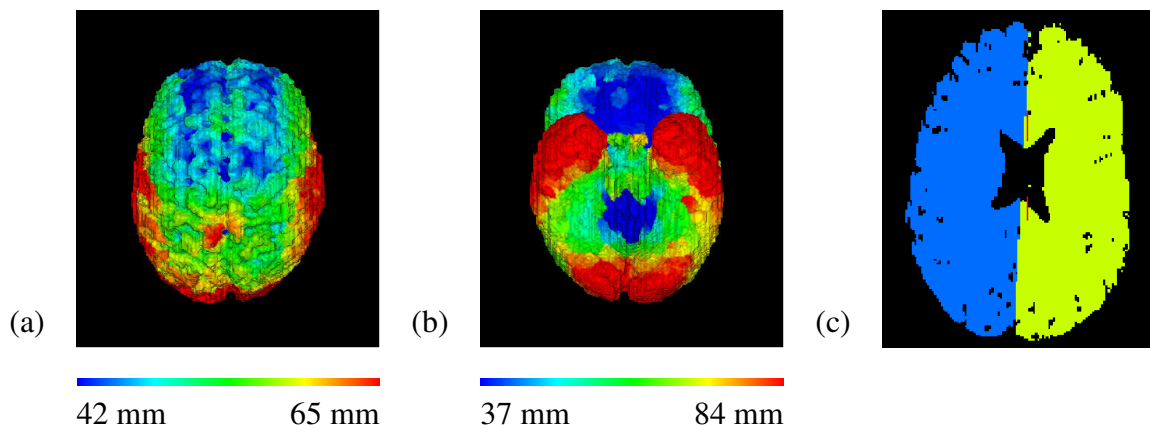


Figure 5. Application on real 3-D datasets: Visualization of distances projected on the cortex from superior (a) and inferior (b) viewpoints, (colormaps adjusted to viewpoint). Visualization of manual segmentations (c) of the hemispheres (blue, yellow) and of the corpus callosum (red) on a slice. There is a mismatch between the inter-hemispheric fissure and the cross-section of the corpus callosum.

Further 3-D tests are still in progress. So far datasets of 10 control patients of an Organic Amnesia study, varying in age and sex, have been processed. Both the corpus callosum and the brain hemispheres were segmented manually. The segmentation of the brain tissues has been performed using statistical classification with the Bayes-classifier. The a-posteriori probabilities were used to calculate the cost matrix. Distances have been visualized (see Figure 5) and there were again significant visual differences between the two hemispheres in all processed datasets. The asymmetry measurements have not yet been calculated. We also observed that the manual segmentation of the corpus callosum is not placed exactly at the location of the interhemispheric fissure for several datasets, resulting in displacements as large as a few millimeters. These displacements are of equal size as the range of the mean differences of the distances for the atlas. As for the test with the atlas we observed again that the correspondence (see Figure 6) should be improved. So far, we did not explicitly determine corresponding brain regions on the two hemisphere to be compared. The result will be significantly improved if a rough correspondence could be established, for example using non-rigid registration [8].

For the processing of one high resolution dataset the computation time was about 20 minutes on a SUN Sparc Ultra 1, including visualization but not including the segmentation of the corpus callosum and the brain tissue.

4. Conclusions and Discussion

In this paper, we have presented a new approach to measure minimum cost paths in a non-Euclidean curvilinear space. We use such paths as a simulation of callosal white matter fiber tracts which are of

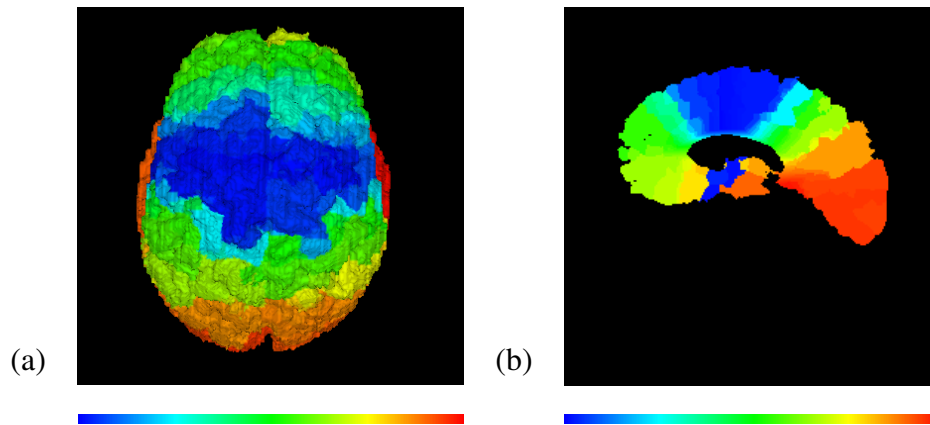


Figure 6. Application on real 3-D datasets: Visualization of the correspondence as projection on the cortex (a) and on a slice (b) close to the interhemispheric fissure in the right hemisphere. Points on the corpus callosum are labeled by a colormap, and labels are projected along optimal paths to the cortex as shown in one sagittal slice.

interest in current neurological research. These paths are calculated as the paths of minimal costs from the white matter boundary to the corpus callosum inside the white matter structure. We also proposed a technique to calculate a rough correspondence and an associated asymmetry measurement. Results are promising, but especially the correspondence needs improvement and we plan to apply a non-rigid registration technique. The method has been applied to 11 3-D dataset so far, and the implementation runs stable and reliable.

The distances determined with our method are based on the city-block metric with the inherent disadvantages of showing large deviations from Euclidean distance measurements and of non-isotropic propagation of distances in space. Kiryati et al. [15] have addressed this issue and have proposed a correction of the calculated distances. We plan to incorporate this correction into a future method. Future directions of our research include the generation of a more robust measurement of asymmetry, combining curvilinear distances with explicitly established lateral correspondence between brain hemispheres. Further, the interactively controlled brain tissue segmentation will soon be replaced by an automatic technique which is an interleaved bias-estimation/tissue classification technique.

Acknowledgments This work was supported by the EC-funded BIOMORPH project 95-0845, a collaboration between the Universities of Kent and Oxford (UK), ETH Zurich (Switzerland), INRIA Sophia Antipolis (France) and KU Leuven (Belgium). Project funding is provided by the Swiss Federal Office for Education and Science (BBW Nr 95.0340).

References

- [1] T.J. Crow. Temporolimbic or transcallosal connections: Where is the primary lesion in schizophrenia and what is its nature ? *Schizophrenia Bulletin*, 23:521–523, 1997.

- [2] T.J. Crow. Schizophrenia as a transcallosal misconnection syndrome. *Schizophrenia Research*, 1998. in print.
- [3] M.E. Shenton. *Psychopathology: The Evolving Science of Mental Disorders*, chapter Temporal lobe structural abnormalities in schizophrenia: A selective review and presentation of new MRI findings, pages 51–99. Cambridge University Press, 1996.
- [4] M.E. Shenton, C.G. Wible, and RW McCarley. *Brain Imaging in Clinical Psychiatry*, chapter MRI studies in schizophrenia, pages 297–380. Marcel Decker Inc., 1997.
- [5] T.J. Crow, N. Colter, C.D. Frith, E.C. Johnstone, and D.G.C. Owens. Developmental arrest of cerebral asymmetries in early onset schizophrenia. *Psych. Res.*, 29:247–253, 1989.
- [6] P. Marais, R. Guillemaud, M. Sakuma, A. Zisserman, and M. Brady. Visualising cerebral asymmetry. In *Proc. of Visualisation in Biomedical Computing*, volume 1131 of *LECTURE NOTES IN COMPUTER SCIENCE*, 1996, pages 411–416. Springer-Verlag, 1996.
- [7] E. Bullmore, M. Brammer, J. Harvey, R. Murray, and M. Ron. Cerebral hemispheric asymmetry revisited: effects of handedness, gender and schizophrenia measured by radius of gyration in magnetic resonance images. *Psychological Medicine*, 25:249–363, 1995.
- [8] S. Prima, J.P. Thirion, G. Subsol, and N. Roberts. Automatic analysis of normal dissymmetry of males and females in mr images. *Proceedings of Medical Image Computing and Computer-Assisted Intervention (MICCAI 98)*, pages 770–779, 1998.
- [9] S. Peled, H. Gudbjartsson, C.F. Westin, R. Kikinis, and F. A. Jolesz. Magnetic resonance diffusion tensor imaging demonstrates direction and asymmetry of human white matter fiber tracts. *Brain research*, 780:27–33, 1998.
- [10] C. Poupon, J.F. Mangin, V. Frouin, J. Régis, F. Poupon, M. Pachot-Clouard, D. Le Bihan, and I. Bloch. Regularization of mr diffusion tensor maps for tracking brain white matter bundles. *Proceedings of Medical Image Computing and Computer-Assisted Intervention (MICCAI 98)*, pages 489–498, 1998.
- [11] M. A. Fischler, J. M. Tenenbaum, and H. C. Wolf. Detection of roads and linear structures in low-resolution aerial imagery using a multisource knowledge integration technique. *Computer Graphics and Image Processing*, 15:201–223, 1981.
- [12] Eric N. Mortensen and William A. Barret. Intelligent scissors for image composition. *Proceedings of Computer Graphics (SIGGRAPH 95)*, pages 191–198, August 1995.
- [13] Eric N. Mortensen and William A. Barret. Fast, accurate, and reproducible live-wire boundary extraction. *Proc. Visualization in Biomedical Computing*, pages 183–192, Sep. 1996.
- [14] J.F. Mangin, J. Régis, and V. Frouhin. Shape bottlenecks and conservative flow systems. *Proceedings of MMBIA*, pages 319–328, 1996.
- [15] Nahum Kiryati and Gábor Székely. Estimating shortest paths and minimal distances on digitized three-dimensional surfaces. *Pattern Recognition*, 26:1623–1637, 1993.